Validation of leading-point-concept-based approach to predicting an increase in turbulent burning rate due to diffusional-thermal effects

Proceedings of the Combustion Institute 42 (2026) 106134

Contents lists available at ScienceDirect

Proceedings of the Combustion Institute

journal homepage: www.elsevier.com/locate/proci

Validation of leading-point-concept-based approach to predicting an increase in turbulent burning rate due to diffusional-thermal effects

Yiqing Wang [a], Van Tinh Mai [b], Zheng Chen [c], Shenqyang (Steven) Shy [b], Andrei N. Lipatnikov [d,*]

[a] Department of Aeronautical and Aviation Engineering, The Hong Kong Polytechnic University, Hong Kong, 999077, China
[b] Department of Mechanical Engineering, National Central University, Taoyuan City, 320317, Taiwan
[c] SKLTCS, HEDPS-CAPT, College of Engineering, Peking University, Beijing, 100871, China
[d] Department of Mechanical Engineering, Chalmers University of Technology, Göteborg, 412 96, Sweden

ARTICLE INFO

Keywords:
Turbulent flame speed
Diffusional-thermal effects
Leading point concept
Experiments
Strained laminar flames

ABSTRACT

A promising approach to predicting a significant increase in turbulent burning rate due to diffusional-thermal phenomena in lean H_2-containing mixtures is based on the leading point concept and consists in substituting characteristics of unstretched laminar flames with the counterpart characteristics of highly strained, twin, counterflow laminar flames. In the present work, the predictive capabilities of this approach are validated by processing two experimental databases obtained recently by independent research groups from (i) piloted, statistically stationary, Bunsen-type lean CH_4/H_2/air weakly turbulent ($Re_T = 64$) flames at Karlovitz numbers ranging from 0.5 to 100 and (ii) statistically spherical turbulent flames expanding in various mixtures (stoichiometric $CH_4/O_2/N_2$, lean $H_2/O_2/N_2$, H_2/O_2/He, and H_2/O_2/Ar) under different pressures and temperatures. In each set of experiments, an increase in the burning velocity, U_T, due to diffusional-thermal effects is well pronounced and the use of standard characteristics of laminar flames to fit the data yields a significant scatter. On the contrary, when adopting the consumption velocities and thicknesses of highly strained laminar counterflow twin flames, computed using detailed chemistry, both databases on U_T are well parameterized.

Novelty and significance statement: Analyses of two recent advanced experimental databases on turbulent burning velocities of lean H_2-containing mixtures demonstrate the capabilities of the leading point concept for predicting a significant increase in turbulent burning rate due to diffusional-thermal effects. These capabilities are demonstrated for two very different flame configurations under a wide range of conditions, including elevated pressures and temperatures. The validation of the leading point concept is significant for modeling turbulent burning of lean mixtures that contain H_2. The concept can be adapted in both Reynolds-Averaged Navier-Stokes and Large Eddy Simulations of turbulent combustion of various lean mixtures, e.g., blends of hydrogen with ammonia, carbon oxide, or methane, in various engines such as piston engines, stationary gas turbines, or aeroengine afterburners.

1. Introduction

Burning carbon-free fuels such as hydrogen is a promising technology for the sustainable transition to zero CO_2 emissions from the energy and transport sectors [1]. For advancing this technology, both experiments and high-fidelity simulations are required. From the perspective of modeling of the combustion of lean mixtures containing hydrogen (H_2), the major fundamental challenge consists in predicting a significant increase in turbulent burning rate due to diffusional-thermal effects [2]. This phenomenon was discovered about 65 years ago [3] and has been documented in many experimental and Direct Numerical Simulation (DNS) studies reviewed elsewhere [4–6], with the effect magnitude being very high [7,8].

While various approaches to modeling such effects have been developed, as reviewed in [4], two of them predominate in the recent literature. One long-known approach that recently received renewed attention [5,6,9] consists in highlighting the diffusional-thermal instability of laminar flames [10]. Another approach is based on the leading

* Corresponding author.
E-mail addresses: lipatn@chalmers.se, andrei.lipatnikov@chalmers.se, lanna616800@gmail.com (A.N. Lipatnikov).

https://doi.org/10.1016/j.proci.2026.106134
Received 6 March 2026; Accepted 6 June 2026
Available online 26 June 2026

point concept [10–12].

Since the two approaches still compete and burning of lean mixtures containing H_2 (e.g., H_2-air, syngas-air, NH_3-H_2-air, or CH_4-H_2-air flames) is a problem of high fundamental and practical importance in combustion science and technology, these approaches urgently require further testing against newly measured data. Two sets of recent experiments [13,14] and [15], performed using different diagnostic techniques in very different flame configurations under different conditions, offer new opportunities for such tests. Accordingly, this work aims to explore the capabilities of the leading point concept and another recent approach [9] for quantitatively predicting the significant increase in turbulent burning rate due to diffusional-thermal effects, documented in the cited experimental studies for various mixtures.

In the next section, the experiments are briefly described and the methods adopted to analyze the measured data are presented. The obtained results are reported in Section 3 and are further discussed in Section 4. Conclusions are drawn in Section 5.

2. Research methods

2.1. Cambridge data

Experiments were conducted with statistically stationary Bunsen-type turbulent flames under room conditions [15]. The bulk turbulent burning velocities $U_T = \dot{m}/(\rho_u A_T)$ were obtained by applying Mie-scattering techniques to measure the areas A_T of mean flame surfaces. Here, $\dot{m}$ is the inlet mass flow rate and ρ_u is the inlet flow density. All measurements were performed in the same weakly-turbulent flow: inlet velocity $U = 3.5$ m/s, rms turbulent velocity $u' = 0.37$ m/s, integral length scale $L = 2.6$ mm, turbulent time scale $\tau_T = L/u' = 7$ ms, and turbulent Reynolds number $Re_T = u'L/\nu_u = 64$, where ν_u is the molecular kinematic viscosity of unburned gases.

The peculiarity of the study consists of the unique design of the mixtures [15]. Specifically, first, five lean CH_4-air mixtures were selected by (i) using the GRI 3.0 chemical mechanism [16] to compute dependencies of the laminar flame speed S_L and thickness $\delta_L = (T_b - T_u)/\max\{|dT/dx|\}$ on the equivalence ratio ϕ and (ii) finding five different values of $0.44 \le \phi \le 0.94$ that yielded five different Karlovitz numbers $Ka = (u'/S_L)^{3/2}(L/\delta_L)^{-1/2} = 0.5$, 1, 5, 20, and 100. Here, T is the temperature; the subscripts u and b refer to unburned reactants and burned products, respectively. Second, for each Ka, a set of H_2-CH_4-air mixtures was designed by (i) increasing the mole fraction χ of hydrogen in CH_4/H_2 blends from 0 to 1 with a step of 0.1 and (ii) simultaneously decreasing ϕ to retain the same computed values of S_L and δ_L and, hence, the same Ka for each mixture set.

In total, 46 mixtures were designed [15, Table 1]. In 14 cases (low S_L and small χ), the flames were tall and were not entirely captured by the applied diagnostic techniques [15, Fig. 6]. For the sake of rigor, these cases are excluded from the following analyses. This restriction is of minor importance for the present goals, because the flames were too tall when U_T was low, i.e., under conditions of a weak increase in burning rate due to diffusional-thermal effects.

Table 1
Major characteristics of Ar-containing mixtures.

ϕ	X_{Ar}			[23]		[24]		σ	Le
		P atm	T_u K	S_L cm/s	δ_L mm	S_L cm/s	δ_L mm		
0.45	5.96	1	300	28.0	0.62	23.5	0.63	4.7	0.35
0.45	4.9	2	300	40.0	0.24	33.5	0.24	5.2	0.36
0.45	5.47	2	300	28.0	0.29	24.0	0.29	4.95	0.36
0.45	4.85	5	300	28.0	0.11	22.5	0.11	5.2	0.36
0.45	6.06	1	400	61.6	0.57	51.9	0.57	3.7	0.35
0.45	5.54	2	400	61.9	0.25	51.4	0.25	3.9	0.36
0.45	4.8	5	400	62.2	0.09	50.9	0.08	4.2	0.36

2.2. National Central University (NCU) data

A different set of experiments [13,14] was conducted in a dual-chamber fan-stirred explosion facility (cruciform burner [17]) using high-speed Schlieren techniques to monitor the growth of a statistically spherical flame kernel in homogeneous isotropic turbulence after spark ignition at the bomb center.

Near-isotropic turbulence is generated in a central domain of 150 × 150 × 150 mm^3 by controlling the fan frequency f (Hz) of a pair of counter-rotating fans and using perforated plates, as described in detail elsewhere [18]. The following empirical relations: $u' = 0.0462f$ (m/s) and $L = 10.7f^{0.34}$ (mm) have been confirmed in LDV and PIV measurements [17,18].

The heating system [19] consists of (i) a set of primary chamber surface heaters with a total power of 17 kW, which heat up the gas in the burner through heat conduction, and (ii) two perforated plate heaters (2.4 kW) used to heat up the gas via more efficient turbulent heat convection. The system enables a uniform temperature field in the domain of measurements, where temperature variations are lower than 1°C [19].

A flame kernel (i) is initiated by discharging ignition energy through two stainless-steel electrodes with sharp ends [20] and (ii) is recorded using the Schlieren imaging technique and a high-speed (10,000 frame/s), high-resolution (800 × 800 pixels) camera.

When processing such Schlieren images, the mean flame radius $\langle R_f \rangle(t) = [A(t)/\pi]^{1/2}$ is measured using the area $A(t)$ enclosed by the wrinkled turbulent flame front contour. Subsequently, the turbulent flame speed $S_T = (\rho_b/\rho_u)d\langle R_f \rangle/dt$ is evaluated by (i) fitting the measured $\langle R_f \rangle(t)$-curves with straight lines in the range of 25 mm $\le \langle R_f \rangle \le$ 35 mm to avoid disturbances due to spark ignition and (ii) averaging the obtained results over five repeated runs under statistically identical conditions. This number of runs is sufficient, because the scatter of measured flame speeds is low at the modest turbulent intensities adopted here.

Previously, stoichiometric CH_4/air and lean ($\phi = 0.45$) $H_2/O_2/N_2$/He turbulent flames were explored by varying the pressure P and adjusting the volume fraction of an inert diluent in the hydrogen mixtures to obtain close values of S_L for the two fuels at the same pressure, while S_L was varied with P [13]. Later, the mole fraction X_{N2} of N_2 in each fuel/O_2/N_2 mixture (still $\phi = 1.0$ for CH_4 and $\phi = 0.45$ for H_2) was adjusted to retain close values of S_L not only for different fuels, but also at different pressures P [14]. Moreover, these experiments were performed at $T_u = 300$ and 400 K (the values of S_L were different at different T_u). Here, the latest [14] set of conditions (12 different X_{N2} for $P = 1$, 2, or 5 atm, $T_u = 300$ or 400 K, and H_2 or CH_4) is extended by adding six more cases based on lean ($\phi = 0.45$) H_2/O_2/Ar mixtures, the same three pressures, and the same two T_u. Argon is used, because its molecular weight is larger than that of O_2 or N_2 and, hence, diffusional-thermal effects are expected to be more pronounced. As before [13,14], mixture compositions were designed based on S_L, which was computed using the PREMIX module [21] of the CHEMKIN-2 package [22] and the GRI mechanism [16] for CH_4 or a mechanism by Kéromnès et al. [23] for H_2. Both multi-diffusion and thermo-diffusion options of PREMIX [21] were used.

In total, nine stoichiometric $CH_4/N_2/O_2$, nine $H_2/N_2/O_2$, seven H_2/O_2/Ar, and three H_2/O_2/He mixtures were studied. The characteristics of the newly designed Ar-containing mixtures are listed in Table 1, where $\sigma = \rho_u/\rho_b$ is the density ratio and the Lewis number Le is defined as the ratio of the mass diffusivity of H_2 to the heat diffusivity of the mixture. The characteristics of other mixtures are reported in Refs. [13, 14]. For each set of T_u, P, and mixture composition, measurements were performed at $u' = 0.5$ and 1 m/s. Accordingly, $0.8 < u'/S_L < 3.6$, $40 < L/\delta_L < 375$, $390 < Re_T < 9500$ and $0.1 < Ka < 45$, with a total of 56 values of U_T being measured.

In addition to the values of S_L and δ_L, computed using a mechanism

by Kéromnès et al. [23], Table 1 also reports results obtained using a mechanism by Konnov [24], with all other things being equal. The latter mechanism is adopted here for the following reasons. Many chemical models used in simulations of laminar flames, including the model by Kéromnès et al. [23], involve the Sandia transport database [25] created using the 12-6 Lennard-Jones potential to calculate diffusion coefficients. In contrast, the model by Konnov [24] involves a new transport property database [26] created by calculating parameters of the 12-6 Lennard-Jones potential from accurate full-dimensional intermolecular potentials and using several first-principle theoretical methods. Such differences in transport properties could play a more important role in mixtures containing He or Ar, which are less studied in the combustion literature than fuel-air mixtures. Accordingly, the chemical model by Konnov [24] will also (in addition to the model by Kéromnès et al. [23]) be used to analyze the NCU data on S_T, including both data reported earlier [13,14] and the new data obtained from mixtures with Ar. The two mechanisms are used to show the weak sensitivity of the major findings to the choice of chemical models.

2.3. Data analyses and underlying concepts

Both sets of experimental data [13,14] and [15] were processed using methods adopted in Refs. [14,27–29]. The methods are based on the following fit:

$$\frac{U_T}{u'} = a\left[\left(\frac{u'}{S}\right)\left(\frac{L}{\delta}\right)^q\right]^b, \tag{1}$$

with different models tested for the speed S and thickness δ. Initially, either the Cambridge database or the NCU database was fitted by (i) using $S = S_L$ and $\delta = \delta_L$, (ii) varying the power exponent q in Eq. (1) with a step $\Delta q = 0.01$, (iii) applying a least square fit to determine $a(q)$ and $b(q)$ for each q, and (iv) selecting q_m, $a(q_m)$, and $b(q_m)$ that minimized scatter:

$$\in = \sum\left\{\ln\left(\frac{U_T}{u'}\right) - \ln a - b\ln\left[\frac{u'}{S}\left(\frac{L}{\delta}\right)^q\right]\right\}^2 \tag{2}$$

Power-law empirical expressions similar to Eq. (1) are widely used to fit experimental data, e.g., see review articles [30–32] or Refs. [33–38] for recent examples. It is worth stressing, however, that the focus of this work is solely on exploring different models for the speed S and thickness δ in Eq. (1), whereas determining power exponents a, b, and q that best fit the analyzed data is beyond the present scope. Such a task is of minor fundamental interest, because the fitting exponents depend on (i) the range of variations in u'/S_L and/or L/δ_L [39], (ii) transient effects [40] (including the growth of the mean flame brush thickness [32], which yields a wide set of speeds $S_T \neq U_T$ of differently defined mean flame surfaces), and (iii) the flame configuration and the methods adopted to measure turbulent flame speed or/and burning velocity [41]. Such fitting exponents are expected to differ substantially for the bulk turbulent burning velocities U_T obtained from statistically stationary Bunsen-type flames [15] and the speeds S_T of expanding turbulent flames [13,14]. For these reasons, the Cambridge and NCU databases are processed separately in the present work. For brevity, a single symbol U_T will sometimes subsume both S_T and U_T in the following despite these two quantities being well known to be fundamentally different characteristics of turbulent flames [3,7,32].

Equation (1) does not allow for diffusional-thermal phenomena. To overcome this limitation, Bradley et al. [31] proposed adding a factor of $Le^{-q_{Le}}$ on the right-hand side of Eq. (1) to approximate the influence of differential diffusion on U_T. In the cited paper, $q_{Le} = 0.3$ was recommended. Subsequently, other values of q_{Le} were reported, e.g., $q_{Le} = 0.5$ [33], 1.0 [35,37,38], 1.24 [34], or even 3.5 [27]. Here, this simple and popular method is not assessed due to the significant (order of magnitude) scatter of published values of q_{Le} and because it lacks a fundamental basis.

The focus of the present analyses is placed on two methods that have such fundamental grounds and consist of substitution of characteristics of unstretched, steady, and one-dimensional laminar flames, i.e., $S = S_L$ and $\delta = \delta_L$ in Eq. (1), with characteristics of highly strained [11,12] or unstable [9] laminar flames.

One method stems from the leading point concept [11,12], which addresses mean (time- or ensemble-averaged) U_T and is based on two hypotheses. First, this U_T is assumed to be controlled by processes localized to the leading edge of the turbulent flame brush. Such a feature is not unique to premixed turbulent flames but is known for a large class of travelling-wave solutions (pulled waves) to convection-diffusion-reaction equations. Such pulled waves were found in various fields of natural science [42,43] since Kolmogorov et al. [44] rigorously proved the so-called KPP theorem. It states that, under certain but not too restrictive conditions, the speed of a travelling wave is controlled by processes localized to the wave leading edge. This theorem was applied to premixed turbulent flames long ago [45,46] and the reader interested in the latest (non-rigorous) extensions of the KPP theorem to turbulent combustion is encouraged to look into Refs. [47–49]. An important role of the leading edge of a premixed turbulent flame brush in its propagation was recently argued from another perspective [50]. It is also worth noting that, under conditions of validity of the KPP theorem, other approaches, e.g., the flame surface density concept of turbulent combustion [51], should yield the same wave speed, but may complement the KPP theorem by describing the wave structure.

Second, critically perturbed (close to quenching) laminar premixed flames were hypothesized [10,11] to model the local burning rate in the leading reaction zones that control turbulent flame expansion. This hypothesis does not mean that such zones move to the leading edge of a turbulent flame brush due to a large increase in the local flame displacement speed. Rather, the hypothesis may imply that such zones are advected to the leading edge by intense turbulent fluctuations [10], with the process being stopped when turbulence upstream of the leading zone is very intense and can locally extinguish combustion. At this critical instance, however, local combustion quenching does not occur, but the leading reaction zone does not propagate further into fresh reactants. In other words, when a flame reaches a region where turbulence is too intense, the flame does not enter this region [11,52], but can still propagate in other directions. Accordingly, leading points in turbulent flows may be associated with critically perturbed laminar flames.

Originally [10,11], critically strained, planar, twin, counter-flow laminar flames [53] were proposed as a simple model that allowed evaluating the local burning rate at leading points. The relevance of such laminar flames to modeling the mean structure of local reaction zones at the leading edge of a turbulent flame brush was shown in recent DNS studies [54–57]. Nevertheless, it is worth stressing that (i) the instantaneous local structure of reaction zone elements characterized by the highest (over the entire flame brush) fuel consumption rate is much more complicated [58,59] and (ii) the appearance of planar, twin, counter-flow laminar flames at the leading edge of a turbulent flame brush has never been documented. This is therefore a simplified model that offers the opportunity to estimate high local burning rates in critically perturbed low Le laminar flames without any tuning.

Thus, within the framework of the leading point concept [10,11], planar, twin, counter-flow laminar flames are simulated to compute the dependence of the following consumption velocity

$$u_c = \frac{W_F}{2\rho_u Y_{F,u}} \int_{-\infty}^{\infty} |\dot{\omega}_c(x)| dx \tag{3}$$

on strain rate g. Here, W_F is the fuel molecular weight; Y_F is the fuel mass fraction; and $\underset{c}{\omega}$ is the fuel consumption rate. In the case of a low Le, such $u_c(g)$-dependencies are monotonously increasing functions, with the exception of a narrow range of g under near-extinction conditions, e.g.,

see Fig. 3 in Section 3. Hence, to avoid tuning, S and δ in Eq. (1) were proposed [13,27–29] to be substituted with $u_c^m = \max\{u_c(g)\}$ and the thickness $\delta_L^m = (T_b - T_u)/\max\{|dT/dx|\}$ evaluated at the same strain rate close to extinction conditions.

At $Le \geq 1$, u_c is reduced by g and the two principles invoked above (maximum u_c and near-quenching conditions) become inconsistent. The present authors are not aware of a cogent explanation of this inconsistency, but the scenario in which turbulent flame propagation is controlled by reaction zones characterized by $u_c < S_L$ appears counterintuitive. In recent applications [13,27–29] of the leading point concept for predicting diffusional-thermal effects on U_T, the principle of maximum u_c was prioritized, i.e., the effects were neglected for mixtures characterized by $u_c(g) \leq S_L$. Since CH_4 is characterized by $Le \approx 1$ and weak diffusional-thermal effects, such a simplified approach appears reasonable for all mixtures considered in the present work, especially since it does not involve tuning constants.

Nevertheless, it is worth stressing that (i) the priority of the maximum u_c principle still requires justification and (ii) the outlined simplified approach may be oversimplified for turbulent flames characterized by large Le. The present authors are not aware of a model with demonstrated capability to predict diffusional-thermal effects on U_T at $Le > 1$, while the magnitude of such effects is much smaller compared to low-Lewis-number mixtures [2,4].

Thus, in the following, Eq. (1) with $S = S_L$ and $\delta = \delta_L$ is adopted for mixtures characterized by $u_c(g) \leq S_L$, while $S = u_c^m$ and $\delta = \delta_L^m$ for other (low Le) mixtures. Consequently, Eq. (1) reduces to

$$\frac{U_T}{u'} = a\left[\left(\frac{u'}{u_c^m}\right)\left(\frac{L}{\delta_L^m}\right)^q\right]^b \tag{4}$$

at low Le. It is worth stressing that transition from Eq. (1) to Eq. (4) is based solely on physical hypotheses. Although some of them still require justification, they do not introduce any additional fitting parameter.

Another approach assessed here is based on (i) theoretical results [60] on the normalized contribution ω_{TD} of diffusional-thermal effects to the growth rate of laminar flame instability in the case of low Le and (ii) a large DNS database obtained from laminar and turbulent flames [9,61]. By analyzing these DNS data, the following "empirical scaling models" [15]

$$s_F = S_L \exp\left(0.08\omega_{TD}^+ \chi^{3.3}\right), \tag{5}$$

$$\delta_F = \delta_L \exp\left(-0.06\omega_{TD}^+ \chi^{3.3}\right), \tag{6}$$

where $\omega_{TD}^+ = \max(\omega_{TD}, 0) \geq 0$, were proposed "to capture the local flame consumption speeds measured in three-dimensional DNS" [15] of H_2/CH_4/air flames. Here, χ is the mole fraction of hydrogen in CH_4/H_2 blends. Accordingly, Eq. (1) could be replaced with

$$\frac{U_T}{u'} = a\left[\left(\frac{u'}{s_F}\right)\left(\frac{L}{\delta_F}\right)^q\right]^b. \tag{7}$$

If a laminar flame is stable with respect to diffusional-thermal effects, $\omega_{TD} < 0$. Hence, $\omega_{TD}^+ = 0$, $s_F = S_L$, and $\delta_F = \delta_L$, i.e., the influence of such effects on U_T is neglected.

In contrast to the leading point concept, this approach is partially empirical, see coefficients 0.08, 0.06, and 3.3 in Eqs. (5) and (6), but it is also based on the state-of-the-art activation-energy-asymptotic theory [60] for laminar premixed flames subject to weak, large-scale (when compared to δ_L) perturbations.

For the sake of rigor, Eqs. (5)-(7) are applied only to Cambridge data in the following, because the ω_{TD} values are reported for all 46 mixtures in Ref. [15].

3. Results

Figures 1a and 2a show that the data on U_T/u' are widely scattered and poorly fitted when using S_L and δ_L in Eq. (1). Comparison of triangles with circles and diamonds in Fig. 1a shows that S_T/u' is significantly lower for $CH_4/O_2/N_2$ mixtures than for $H_2/O_2/N_2$ or H_2/O_2/Ar mixtures. This difference is attributed to diffusional-thermal effects.

On the contrary, both the NCU and Cambridge data are well fitted with the following forms of Eq. (4)

$$\frac{S_T}{u'} = 0.75\left(\frac{u'}{u_c^m}\right)^{-0.63}\left(\frac{L}{\delta_L^m}\right)^{0.14}, \tag{8}$$

$$\frac{U_T}{u'} = 1.86\left(\frac{u'}{u_c^m}\right)^{-0.73}\left(\frac{L}{\delta_L^m}\right)^{0.1}, \tag{9}$$

see Figs. 1b and 2b, respectively. These results were obtained using chemical models from Refs. [24] and [16], respectively. In both figures, the symbols collapse well onto the fitting lines independently of the fuel formula, ϕ, inert diluent, pressure, temperature, etc. The coefficients of determination R^2 reported in Figs. 1b and 2b are 0.931 and 0.95, respectively.

Calculations of u_c^m and δ_L^m in Eqs. (8) and (9) are illustrated using pentagons in Fig. 3, where typical results of simulations of stationary, planar, twin, counterflow laminar premixed flames are shown. These results have been obtained for selected mixtures from the Cambridge database [15] using Cantera [62] and the GRI 3.0 mechanism [16] with a multicomponent transport model including the Soret effect. Comparison of Figs. 3b and 3c illustrates the evaluation of the thickness δ_L^m. Similar results were computed for other H_2/CH_4/air mixtures. For the NCU database, dependencies of u_c/S_L on Ka_S are similar to the curves plotted in Figs. 3a and 3b, e.g., see [14, Fig. 4], and are not reported here. Fitting results obtained using two chemical models [23,24] are

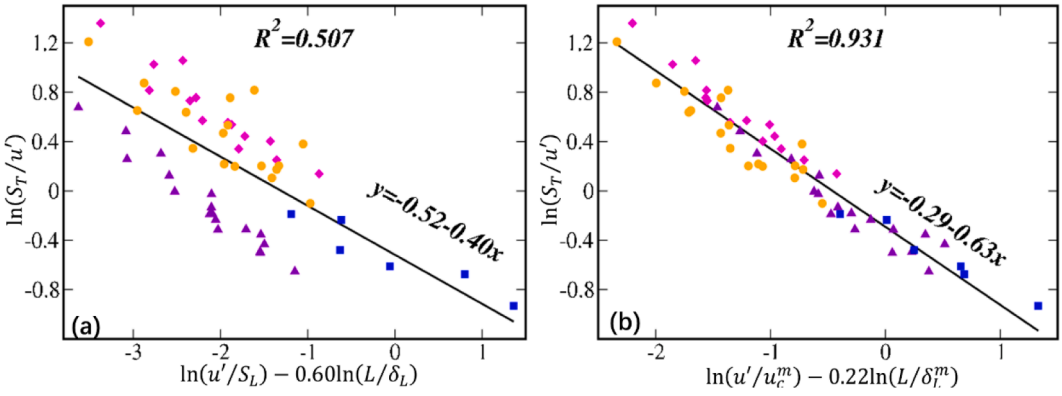

Fig. 1. Results of fitting NCU data using (a) Eq. (1) and (b) Eq. (8). Violet triangles, blue squares, orange circles, and magenta diamonds show data obtained from CH_4/air, H_2/O_2/He, $H_2/O_2/N_2$, and H_2/O_2/Ar flames, respectively. $0.8 < u'/S_L < 3.6$, $40 < L/\delta_L < 375$, $1 \leq u_c^m/S_L < 7.4$, $0.19 < \delta_L^m/S_L \leq 1$.

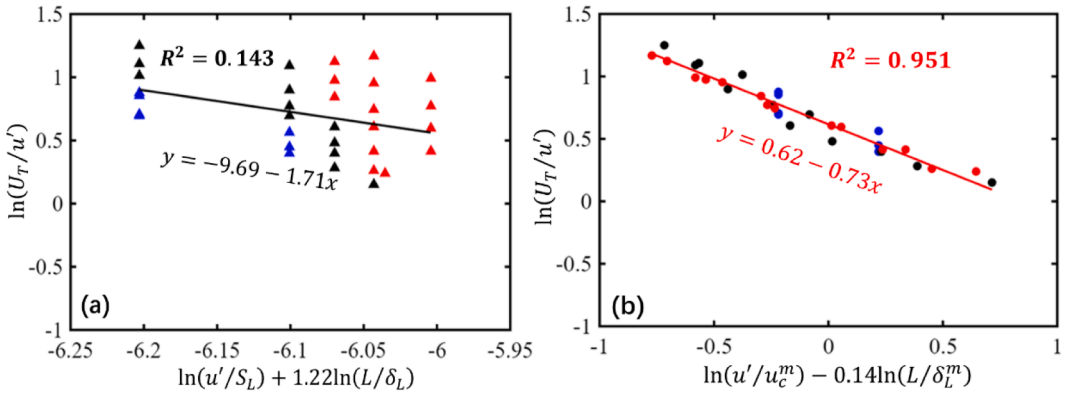

Fig. 2. Results of fitting Cambridge data using (a) Eq. (1) and (b) Eq. (9). Blue, black, and red symbols show data measured at $\{\omega_{TD} < 0; u_c^m = S_L\}$, $\{\omega_{TD} < 0;\ u_c^m > S_L\}$, and $\{\omega_{TD} > 0; u_c^m > S_L\}$, respectively. $0.8 < u'/S_L < 18$, $0.8 < L/\delta_L < 7.6$.

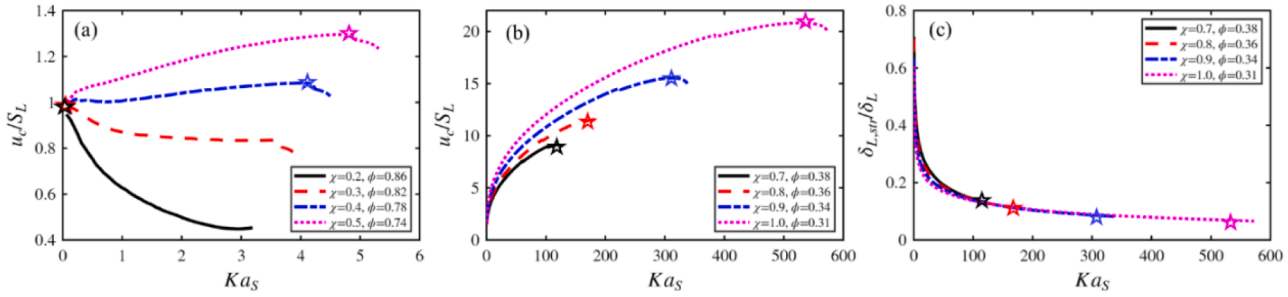

Fig. 3. Results of simulations of twin counterflow laminar flames for certain mixtures explored in Cambridge experiments [15]. (a) and (b) normalized consumption velocity vs. normalized strain rate $Ka_S = g\delta_L/S_L$ in cases of $Ka = 0.5$ and 100, respectively. (c) normalized flame thickness vs. Ka_S in cases of $Ka = 100$. Mixture compositions are specified in legends.

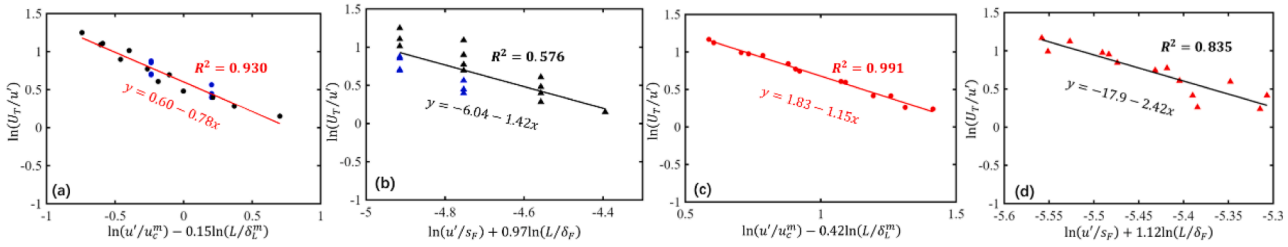

Fig. 4. Cambridge data obtained from flames characterized by (a)-(b) $\omega_{TD} < 0$ or (c)-(d) $\omega_{TD} > 0$. Results obtained using Eqs. (4) or (7) are shown in (a) and (c) or (b) and (d), respectively. Symbol colors are explained in captions to Fig. 2.

also similar, see Fig. S1 in the Supplementary Material, although there are quantitative differences even for S_L, see Table 1. Figures 1 and S1 show that the good performance of Eq. (4) is weakly sensitive to the chemical model invoked.

Since the performance of the GRI 3.0 mechanism for H_2/CH_4/air flames (Cambridge data) may be questioned, simulations were also performed using the Foundational Fuel Chemistry Model (FFCM-1) [63] for, with all other conditions (software and transport models) being equal. The results obtained using these chemical models are similar, e.g., substitution of u_c^m and δ_L^m, computed using FFCM-1 model, into Eq. (4) yields $R^2 = 0.931$. The latter results are shown in Fig. S2 in the Supplementary Material.

Figure 3a indicates that u_c decreases with increasing strain rate in moderately lean mixtures with small χ. In such cases, $u_c^m = S_L$ and $\delta_L^m = \delta_L$ in Eq. (4). In many other lean cases, e.g., $\chi \geq 0.4$ and $\phi \leq 0.78$ in Fig. 3a, $u_c^m/S_L > 1$ and increases with χ, with these flames surviving under higher strain rates at a larger χ. Thus, diffusional-thermal effects are well pronounced in these mixtures.

Contrary to the $u_c(Ka_s)$-dependencies plotted in blue dotted-dashed and magenta dotted lines in Fig. 3a, Eqs. (5)-(7) do not predict any diffusional-thermal effect for Cambridge flames characterized by $Ka = 0.5$. Indeed, $\omega_{TD} < 0$ in all these flames [15] (Table 1). Hence, $\omega_{TD}^{+} = 0$, $s_F = S_L$, and $\delta_F = \delta_L$. Figure 4b confirms that Eqs. (5)-(7) poorly fit the data measured in cases of $\omega_{TD} < 0$ (not only at $Ka = 0.5$, but also at $Ka = 1$, 5, or 20, see different columns of symbols), while these data show diffusional-thermal effects (an increase in U_T with increasing χ and decreasing Le).

Comparison of blue ($\omega_{TD} < 0, u_c^m = S_L$) and black ($\omega_{TD} < 0,\ u_c^m > S_L$) triangles in Fig. 4b shows that U_T/u' is larger for mixtures characterized by $u_c^m > S_L$. Accordingly, Fig. 4a indicates that this reduced ($\omega_{TD} < 0$) database is well fitted by Eq. (4) and there is no difference between flames associated with $u_c^m = S_L$ (black circles) or $u_c^m > S_L$ (blue circles).

Figure 4c shows that Eq. (4) very well fits U_T measured in mixtures characterized by $\omega_{TD} > 0$ also. The same data are approximated less accurately with Eq. (7), see Fig. 4d. While the use of s_F and δ_F results in significantly better fitting, cf. red triangles in Figs. 2a and 4d, the

performance of Eq. (4) is still superior.

The reason is that the values of u_c^m, computed as shown in Fig. 3, are significantly higher than s_F yielded by Eq. (7) for lean mixtures characterized by a low Lewis number, see Fig. 5. This difference is particularly large for flames associated with $\omega_{TD} > 0$, low *Le*, and large *Ka* (due to low S_L), see Fig. 5b.

Figure 6 shows dependencies of the normalized turbulent burning velocity U_T/S_L, peak consumption velocity u_c^m/S_L, and growth rate ω_{TD} on the Zel'dovich number $Ze = \Theta(T_b - T_u)/T_b^2$. The activation temperature Θ was evaluated by computing laminar flame speeds for mixtures diluted with a small amount of N_2, as discussed elsewhere [64]. In line with recent experimental [13,14] and DNS data [9,65], U_T/S_L increases with *Ze*, with this correlation being well pronounced, see Fig. 6a (note that the use of the ratio Ze/Pe introduced in Ref. [65] yields a much weaker correlation). The dependence of u_c^m/S_L on *Ze* is very similar to that of U_T/S_L, cf. Figs. 6b and 6a, respectively. On the contrary, the correlation between ω_{TD} and *Ze* is significantly weaker, see Fig. 6c. Thus, Fig. 6 further indicates that u_c^m/S_L is more relevant for parameterizing the discussed experimental data on U_T/S_L. Nevertheless, one should bear in mind that there is noticeable uncertainty in computing *Ze* [66].

4. Discussion

The poorer performance of the ω_{TD}-based approach [9] may be attributed to at least two factors. First, the theoretical equations for ω_{TD} [60], derived for single-step-chemistry flames in the high-activation-energy asymptotic limit, are unlikely to hold for complex-chemistry flames characterized by finite activation energies. A similar issue is well known for the growth rate of hydrodynamic instability of laminar flames in the case of $Le \approx 1$ [67,68]. Hence, a method for evaluating ω_{TD} for complex-chemistry unstable laminar flames should be elaborated.

Second, the utility of characteristics of unstable laminar flames for predicting an increase in U_T due to diffusional-thermal phenomena remains unclear. As discussed elsewhere [57], (i) many local or global characteristics of unstable laminar and turbulent lean H_2-air flames differ significantly and (ii) diffusional-thermal phenomena manifest in multiple ways, with diffusional-thermal instability being only one of them. The prioritization of this instability over other manifestations of diffusional-thermal effects requires justification.

In this regard, the following fundamental difference between the two approaches compared is worth emphasizing. They deal with opposite types of local flame perturbations. Indeed, the leading point concept highlights highly perturbed (near-quenching) reaction zones, whereas the key quantity in Eqs. (5) and (6), i.e., the growth rate ω_{TD}^+, has been introduced by studying laminar flame instability, i.e., the response of a laminar flame to infinitesimal perturbations. It is therefore not surprising that u_c^m/S_L, which characterizes the local increase in burning rate in highly perturbed reaction zones, is much larger than s_F/S_L, which is based on the theory of laminar flames subject to infinitesimal perturbations. Comparison of Figs. 4c and 4d implies that large u_c^m/S_L is more relevant for parameterizing the Cambridge database even for low-*Le* mixtures susceptible to diffusional-thermal instability.

Moreover, the assumption that characteristics of the response of laminar flames to infinitesimal perturbations are relevant for modeling flame dynamics under the influence of large perturbations induced by turbulent eddies is not obvious.

There is also a common limitation of the two approaches. Both are based on the influence of large-scale (with respect to δ_L) perturbations on a laminar flame. Indeed, the classical model [53] of twin, counter-flow laminar flames and the theory [60] of unstable laminar flames address flow perturbations whose length scales are much larger than δ_L. It is not yet clear under which conditions this limitation becomes crucial. This issue requires study.

Nevertheless, the present analyses indicate that, despite this limitation, a significant increase in turbulent burning velocity due to diffusional-thermal effects can be accurately predicted using Eq. (4) and results of complex-chemistry simulations of highly strained, stationary, planar, twin, counter-flow laminar flames. This finding, also supported by recent analyses of experimental [27] and DNS [28,29] data, can be readily applied in multi-dimensional computations of premixed turbulent combustion within both Reynolds-Averaged Navier-Stokes (RANS) and Large Eddy Simulation (LES) frameworks. Indeed, to predict the increase in U_T due to diffusional-thermal effects, one can substitute S_L and δ_L with u_c^m and δ_L^m, respectively, in relevant model equations (if the model selected involves S_L and/or δ_L). A recent example of such RANS computations is given in Ref. [69].

Admittedly, this simple method does not resolve all issues. The use of $u_c^m = S_L$ in cases where $u_c(g) < S_L$ requires further explanation. The prediction of turbulent flame brush thickness, mean concentration fields, emissions, etc., also deserves special attention. For these purposes, alternative approaches may be required. Nevertheless, the ability to quantitatively predict a significant increase in turbulent burning velocity due to diffusional-thermal effects represents an important step forward, because U_T is the primary fundamental characteristic of premixed turbulent flames, and no alternative approach with comparable predictive capability is currently known.

5. Conclusions

The capabilities of the leading-point-concept-based approach (i.e., the substitution of characteristics of unstretched laminar flames with those of highly strained twin counterflow laminar flames) for predicting a significant increase in turbulent burning rate due to diffusional-thermal effects were demonstrated by analyzing two experimental databases obtained recently by two independent research groups from (i)

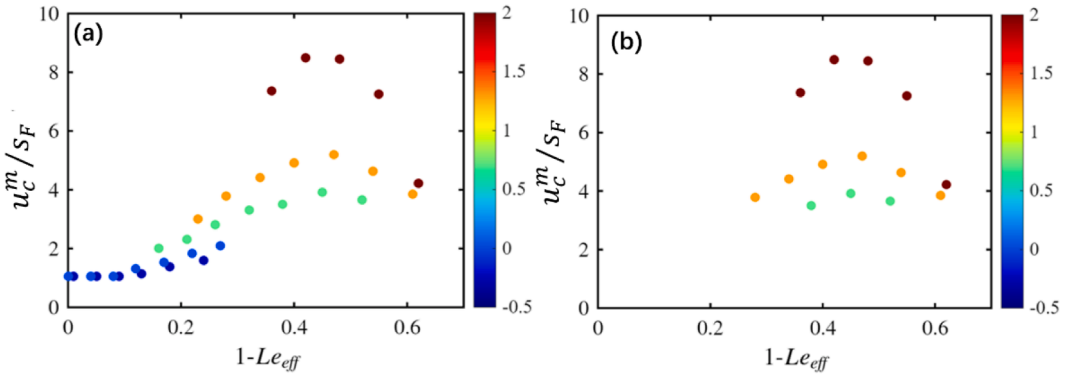

Fig. 5. Ratio of u_c^m/s_F vs. Lewis number reported in Ref. [15]. (a) all Cambridge flames analyzed here, (b) Cambridge flames characterized by $\omega_{TD} > 0$. Color scales show $\log_{10}Ka$, with the values of *Ka* being taken from Ref. [15].

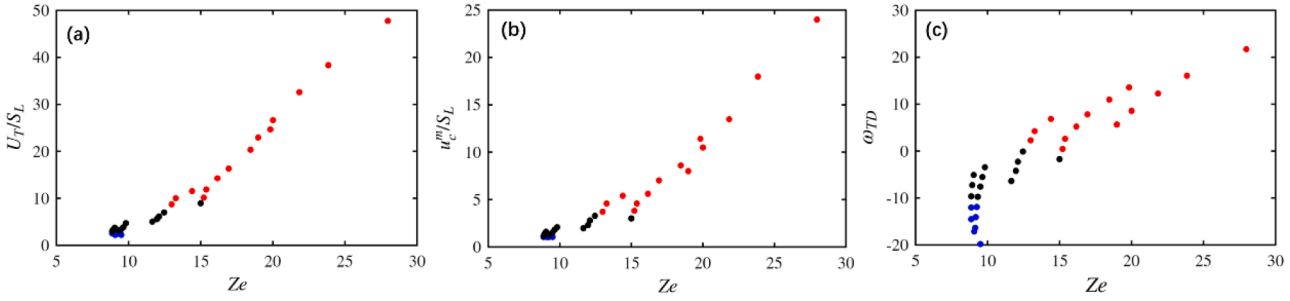

Fig. 6. Dependencies of (a) normalized turbulent burning velocity U_T/S_L, (b) normalized peak consumption velocity u_c^m/S_L in planar twin counter-flow laminar flames, and (c) normalized contribution ω_{TD} of diffusional-thermal effects to growth rate of the flame instability on Zel'dovich number *Ze*. Color scales are explained in captions to Fig. 2.

piloted, statistically stationary, Bunsen-type lean CH_4/H_2/air turbulent flames at Karlovitz numbers ranging from 0.5 to 100 [15] and (ii) statistically spherical flames expanding in various mixtures (stoichiometric $CH_4/O_2/N_2$, lean $H_2/O_2/N_2$, H_2/O_2/He, and H_2/O_2/Ar) under different pressures and temperatures [13,14]. In both sets of measurements, the tested approach, i.e., the use of Eq. (4) instead of Eq. (1), results in collapsing data obtained from different mixtures onto a single curve, with the goodness of fit being high ($R^2 > 0.93$) and weakly sensitive to chemical models invoked.

CRediT authorship contribution statement

Yiqing Wang: Writing – review & editing, Investigation, Formal analysis, Data curation. **Van Tinh Mai:** Writing – review & editing, Investigation, Data curation. **Zheng Chen:** Writing – review & editing, Supervision, Funding acquisition. **Shenqyang (Steven) Shy:** Writing – review & editing, Methodology, Investigation, Funding acquisition. **Andrei N. Lipatnikov:** Writing – original draft, Methodology, Investigation, Funding acquisition, Formal analysis, Conceptualization.

Declaration of competing interest

The authors declare that they have no known competing financial interests or personal relationships that could have appeared to influence the work reported in this paper.

Acknowledgements

The authors are grateful to Prof. S. Hochgreb for sharing the Cambridge experimental database. YW acknowledges financial support by the PolyU Start-up Fund (grant P0060144). ZC acknowledges financial support by the National Natural Science Foundation of China (grant 52425604). SSS acknowledges financial support by National Science and Technology Council, Taiwan (grants 114-2221-E-008-036 and 114-2218-E-008-005). ANL acknowledges financial support by Swedish Research Council (grant 2023-04407).

Supplementary materials

Supplementary material associated with this article can be found, in the online version, at doi:10.1016/j.proci.2026.106134.

References

[1] A. Dreizler, H. Pitsch, V. Scherer, C. Schulz, J. Janicka, The role of combustion science and technology in low and zero impact energy transformation processes, Appl. Energy Combust. Sci. 7 (2021) 100040.
[2] A. Lipatnikov, Fundamentals of premixed turbulent combustion, CRC Press, Florida, 2012.
[3] V.P. Karpov, A.S. Sokolik, Inflammation limits in turbulized gas mixtures, Dokl. Akad. Nauk SSSR 141 (2) (1961) 393–396.
[4] A.N. Lipatnikov, J. Chomiak, Molecular transport effects on turbulent flame propagation and structure, Prog. Energy Combust. Sci. 31 (2005) 1–73.
[5] S. Hochgreb, How fast can we burn, 2.0? Proc. Combust. Inst. 39 (2023) 2077–2105.
[6] H. Pitsch, The transition to sustainable combustion: Hydrogen-and carbon-based future fuels and methods for dealing with their challenges, Proc. Combust. Inst. 40 (2024) 105638.
[7] V.P. Karpov, E.S. Severin, Effects of molecular-transport coefficients on the rate of turbulent combustion, Combust. Explos. Shock. Waves 16 (1) (1980) 41–46.
[8] S. Yang, A. Saha, W. Liang, F. Wu, C.K. Law, Extreme role of preferential diffusion in turbulent flame propagation, Combust. Flame 188 (2018) 498–504.
[9] T.L. Howarth, E.F. Hunt, A.J. Aspden, Thermodiffusively-unstable lean premixed hydrogen flames: Phenomenology, empirical modelling, and thermal leading points, Combust. Flame 253 (2023) 112811.
[10] Ya.B. Zeldovich, G.I. Barenblatt, V.B. Librovich, G.M. Makhviladze, The mathematical theory of combustion and explosions, Plenum, New York, 1985.
[11] V.R. Kuznetsov, Limiting laws of propagation of a turbulent flame, Combust. Explos. Shock Waves 18 (1982) 172–179.
[12] V.R. Kuznetsov, V.A. Sabel'nikov, Turbulence and combustion, Hemisphere Publ. Corp., New York, 1990.
[13] A.N. Lipatnikov, Y.R. Chen, S.S. Shy, An experimental study of the influence of Lewis number on turbulent flame speed at different pressures, Proc. Combust. Inst. 39 (2023) 2339–2347.
[14] H.-Y. Hsieh, S.M. Mousavi, A.N. Lipatnikov, S.S. Shy, Experimental study of the influence of Lewis number, laminar flame thickness, temperature, and pressure on turbulent flame speed using hydrogen and methane fuels, Proc. Combust. Inst. 40 (2024) 105752.
[15] O. Chaib, J. Bae, L. Weller, A. Aspden, S. Hochgreb, Normalization reveals role of thermodiffusive effects in turbulent premixed hydrogen flames, Combust. Flame 286 (2026) 114852.
[16] G.P. Smith, D.M. Golden, M. Frenklach, N.W. Moriarty, B. Eiteneer, M. Goldenberg, C.T. Bowman, R.K. Hanson, S. Song, J.W.C. Gardiner, V.V. Lissianski, Z. Qin, GRI-Mech 3 (1999).
[17] C.C. Liu, S.S. Shy, H.C. Chen, M.W. Peng, On interaction of centrally-ignited, outwardly-propagating premixed flames with fully-developed isotropic turbulence at elevated pressure, Proc. Combust. Inst. 33 (2011) 1293–1299.
[18] T.S. Yang, S.S. Shy, Two-way interaction between solid particles and homogeneous air turbulence: particle settling rate and turbulence modification measurements, J. Fluid Mech. 526 (2005) 171–216.
[19] L.J. Jiang, S.S. Shy, W.Y. Li, H.M. Huang, M.T. Nguyen, High-temperature, high-pressure burning velocities of expanding turbulent premixed flames and their comparison with Bunsen-type flames, Combust. Flame 172 (2016) 173–182.
[20] S.S. Shy, Spark ignition transitions in premixed turbulent combustion, Prog. Energy Combust. Sci. 98 (2023) 101099.
[21] R.J. Kee, J.F. Crcar, M.D. Smooke, J.A. Miller, PREMIX: A FORTRAN Program For Modeling Steady Laminar One-Dimensional Premixed Flames, Sandia National Laboratories, 1989. Report No SAND-89-8249.
[22] R.J. Kee, F.M. Rupley, J.A. Miller, CHEMKIN-II: A FORTRAN Chemical Kinetics Package for the Analysis of Gas-Phase Chemical Kinetics, Sandia National Laboratories, 1989. Report No. SAND-89-8009.
[23] A. Kéromnès, W.K. Metcalfe, K.A. Heufer, N. Donohoe, A.K. Das, C.-J. Sung, J. Herzler, C. Naumann, P. Griebel, O. Mathieu, M.C. Krejci, E.L. Petersen, W. J. Pitz, H.J. Curran, An experimental and detailed chemical kinetic modeling study of hydrogen and syngas mixture oxidation at elevated pressures, Combust. Flame 160 (2013) 995–1011.
[24] A.A. Konnov, Yet another kinetic mechanism for hydrogen combustion, Combust. Flame 203 (2019) 14–22.
[25] R.J. Kee, G. Dixon-Lewis, J. Warnatz, M.E. Coltrin, J.A. Miller, A Fortran computer code package for the evaluation of gas-phase multicomponent transport properties, Sandia National Laboratories, 1986. Report No. SAND86-8246.
[26] A.W. Jasper, J.A. Miller, Lennard-Jones parameters for combustion and chemical kinetics modeling from full-dimensional intermolecular potentials, Combust. Flame 161 (2014) 101–110.
[27] Z. Wang, X. Li, T. Li, A. Dreizler, S.M. Mousavi, A.N. Lipatnikov, B. Zhou, Experimental investigation of NH_3/H_2 jet flames adopting multi-scalar imaging:

Comparison of turbulent burning velocities obtained using different flame-front markers, Combust. Flame 275 (2025) 114054.
[28] Y. Wang, A.N. Lipatnikov, Z. Chen, Characterizing the influence of thermodiffusive effects on turbulent burning velocity of lean hydrogen/air mixtures using critically stretched laminar flames, Combust. Flame 279 (2025) 114306.
[29] S.M. Mousavi, A.N. Lipatnikov, Comment on paper "Flame-turbulence interactions in lean hydrogen flames: Implications for turbulent flame speed and fractal modelling" by F.A. Meziat Ramirez, Q. Douasbin, O. Dounia, O. Vermorel, T. Jaravel, Combustion and Flame 273 (2025) 113926. Combust. Flame 283 (2026) 114592.
[30] R. Abdel-Gayed, K. Al-Khishali, D. Bradley, Turbulent burning velocities and flame straining in explosions, Proc. R. Soc. London A 391 (1984) 393–414.
[31] D. Bradley, A. Lau, M. Lawes, Flame stretch rate as a determinant of turbulent burning velocity, Phil. Trans. R. Soc. London A 338 (1992) 359–387.
[32] A.N. Lipatnikov, J. Chomiak, Turbulent flame speed and thickness: phenomenology, evaluation, and application in multi-dimensional simulations, Prog. Energy Combust. Sci. 28 (2002) 1–74.
[33] M. Nguyen, D. Yu, S. Shy, General correlations of high pressure turbulent burning velocities with the consideration of Lewis number effect, Proc. Combust. Inst. 37 (2019) 2391–2398.
[34] X. Cai, J. Wang, Z. Bian, H. Zhao, M. Zhang, Z. Huang, Self-similar propagation and turbulent burning velocity of CH_4/H_2/air expanding flames: Effect of Lewis number, Combust. Flame 212 (2020) 1–12.
[35] S. Wang, A.M. Elbaz, O.Z. Arab, W.L. Roberts, Turbulent flame speed measurement of NH_3/H_2/air and CH_4/air flames and a numerical case study of NO emission in a constant volume combustion chamber (C.V.C.C.), Fuel 332 (2023) 126152.
[36] S. Zitouni, P. Brequigny, C. Mounaïm-Rousselle, Turbulent flame speed and morphology of pure ammonia flames and blends with methane or hydrogen, Proc. Combust. Inst. 39 (2023) 2269–2278.
[37] S. Wang, A.M. Elbaz, G. Wang, Z. Wang, W.L. Roberts, Turbulent flame speed of $NH_3/CH_4/H_2/H_2O$/air-mixtures: Effects of elevated pressure and Lewis number, Combust. Flame 247 (2023) 112488.
[38] H. Dai, J. Wang, S. Su, L. Su, X. Cai, Z. Huang, Turbulent burning velocity of hydrogen/*n*-heptane/air propagating spherical flames: Effects of hydrogen content, Combust. Flame 260 (2024) 113248.
[39] R. Yu, A.N. Lipatnikov, DNS study of dependence of bulk consumption velocity in a constant-density reacting flow on turbulence and mixture characteristics, Phys. Fluids 29 (2017) 065116.
[40] R. Yu, A.N. Lipatnikov, DNS study of sensitivity of scaling exponents for premixed turbulent consumption velocity to transient effects, Flow, Turbul. Combust. 102 (2019) 679–698.
[41] S. Verma, A.N. Lipatnikov, Does sensitivity of measured scaling exponents for turbulent burning velocity to flame configuration prove lack of generality of notion of turbulent burning velocity? Combust. Flame 173 (2016) 77–88.
[42] U. Ebert, W. van Saarloos, Front propagation into unstable states: universal algebraic convergence towards uniformly translating pulled fronts, Physica D 146 (2000) 1–99.
[43] J.D. Murray, Mathematical biology. 1. An introduction, 3rd ed., Springer, Berlin, 2002.
[44] A.N. Kolmogorov, I. Petrovsky, N. Piskounov, A study of the diffusion equation with a source term and its application to a biological problem, Bjull. MGU A 1 (6) (1937) 1–26.
[45] K.N.C. Bray, P.A. Libby, Interaction effects in turbulent premixed flames, Phys. Fluids 19 (1976) 1687–1701.
[46] B. Hakberg, A.D. Gosman, Analytical determination of turbulent flame speed from combustion models, Proc. Combust. Inst. 20 (1984) 225–232.
[47] V.A. Sabelnikov, A.N. Lipatnikov, Transition from pulled to pushed fronts in premixed turbulent combustion: theoretical and numerical study, Combust. Flame 162 (2015) 2893–2903.
[48] V.A. Sabelnikov, N.N. Petrova, A.N. Lipatnikov, Analytical and numerical study of travelling waves using the Maxwell-Cattaneo relaxation model extended to reaction-advection-diffusion systems, Phys. Rev. E 94 (2016) 042218.
[49] S. Somappa, V. Acharya, T. Lieuwen, Finite flame thickness effects on Kolmogorov-Petrovsky-Piskunov turbulent burning velocities, Phys. Rev. E 106 (2022) 055107.
[50] J.R. Mayo, A.R. Kerstein, Log-correlated large-deviation statistics governing Huygens fronts in turbulence, J. Stat. Phys. 176 (2019) 456–477.
[51] A. Trouvé, T. Poinsot, Evolution equation for flame surface density in turbulent premixed combustion, J. Fluid Mech. 278 (1994) 1–31.
[52] C.K. Law, C.J. Sung, Structure, aerodynamics, and geometry of premixed flamelets, Prog. Energy. Combust. Sci. 26 (2000) 459–505.
[53] A.M. Klimov, Laminar flame in a turbulent flow, Prikladnoy Mekhaniki Tekhnicheskoy Fiziki Zhurnal (USSR) 3 (1963) 49–58.
[54] H. Lee, P. Dai, M. Wan, A.N. Lipatnikov, Influence of molecular transport on burning rate and conditioned species concentrations in highly turbulent premixed flames, J. Fluid Mech. 928 (2021) A5.
[55] H.C. Lee, P. Dai, M. Wan, A.N. Lipatnikov, A numerical support of leading point concept, Int. J. Hydrogen Energy 47 (2022) 23444–23461.
[56] H.C. Lee, A. Abdelsamie, P. Dai, M. Wan, A.N. Lipatnikov, Influence of equivalence ratio on turbulent burning velocity and extreme fuel consumption rate in lean hydrogen-air turbulent flames, Fuel 327 (2022) 124969.
[57] H.C. Lee, B. Wu, P. Dai, M. Wan, A.N. Lipatnikov, Comparison of characteristics of unstable laminar and turbulent lean hydrogen-air flames, Phys. Fluids 37 (2025) 085182.
[58] H.C. Lee, P. Dai, M. Wan, A.N. Lipatnikov, A DNS study of extreme and leading points in lean hydrogen-air turbulent flames - part I: Local thermochemical structure and reaction rates, Combust. Flame 235 (2022) 111716.
[59] H.C. Lee, P. Dai, M. Wan, A.N. Lipatnikov, A DNS study of extreme and leading points in lean hydrogen-air turbulent flames - part II: Local velocity field and flame topology, Combust. Flame 235 (2022) 1117162.
[60] M. Matalon, C. Cui, J.K. Bechtold, Hydrodynamic theory of premixed flames: effects of stoichiometry, variable transport coefficients and arbitrary reaction orders, J. Fluid Mech. 487 (2003) 179–210.
[61] T.L. Howarth, M.S. Day, H. Pitsch, A.J. Aspden, Thermal diffusion, exhaust gas recirculation and blending effects on lean premixed hydrogen flames, Proc. Combust. Inst. 40 (2024) 105429.
[62] D. Goodwin, H. Moffat, R. Speth, Cantera. http://www.cantera.org, 2015.
[63] G. P. Smith, Y. Tao, H. Wang, Foundational Fuel Chemistry Model Version 1.0 (FFCM-1), https://web.stanford.edu/group/haiwanglab/FFCM1/pages/FFCM1.html.
[64] Y. Wang, C. Xu, C. Chi, Y. Yang, Z. Chen, Temperature effect on turbulent burning velocity of lean premixed hydrogen/air flames, Phys. Fluids 36 (2024) 125165.
[65] M. Rieth, A. Gruber, J.H. Chen, The effect of pressure on lean premixed hydrogen-air flames, Combust. Flame 250 (2023) 112514.
[66] T. Lehmann, L. Berger, T.L. Howarth, M. Gauding, S. Girhe, B. Dally, H. Pitsch, Comprehensive linear stability analysis for intrinsic instabilities in premixed ammonia/hydrogen/air flames, Combust. Flame 273 (2025) 113927.
[67] D. Bradley, Instabilities and flame speeds in large-scale premixed gaseous explosions, Phil. Trans. R. Soc. London 357 (1999) 3567–3581.
[68] R. Addabbo, J.K. Bechtold, M. Matalon, Wrinkling of spherically expanding flames, Proc. Combust. Inst. 29 (2002) 1527–1535.
[69] S. Verma, F. Monnier, A.N. Lipatnikov, Validation of leading point concept in RANS simulations of highly turbulent lean syngas-air flames with well-pronounced diffusional-thermal effects, Int. J. Hydrogen Energy 46 (2021) 9222–9233.